



# EXPERIMENTAL PERFORMANCE OF AN R410A-FILLED C-SHAPE THERMOSYPHON

K.S. Ong<sup>a\*</sup>, Gabriel Goh<sup>a</sup>, K.H. Tshai<sup>a</sup>, W.M. Chin<sup>b</sup>

<sup>a</sup>Industrial Engineering Dept., Universiti Tunku Abdul Rahman, 31900 Kampar, Perak, Malaysia.

<sup>b</sup>Daikin Research & Development Malaysia Sdn. Bhd., Taman Perindustrian Bukit Rahman Putra, 47000 Sungai Buloh, Selangor, Malaysia.

## ABSTRACT

Heat pipe heat exchangers (HPHEs) can be used to enhance dehumidification and increase the cooling capabilities of heating, ventilation and air conditioning (HVAC) systems. A C-shape thermosyphon (CST) is a thermosyphon bent into the shape of a “C”. The slope of the CST is defined as the angle of the plane containing the CST to the horizontal. This paper reports on the experimental thermal performance of a R410A-filled CST operating with various power inputs and at various angles of slope. The results show that there is a decrease in performance at 30°. Comparison with results predicted and based on heat transfer coefficients obtained from tests carried out on the vertical thermosyphon showed good agreement.

**Keywords:** Thermosyphon, R410A, C-shape thermosyphon, slope, power input

## 1. INTRODUCTION

In a typical air conditioning system, the supply air would be chilled to below the dew point temperature in the refrigeration machine in order to remove moisture and reduce its humidity. The cold dry air requires reheating to a comfortable design value before it is discharged into the room. Energy is thus required to pre-cool the incoming fresh air and to reheat the supply air. The heat exchange before and after the cooling coil can be performed by using a heat exchanger. In this case, energy needs to be supplied to power the recirculating pump. Heat pipe heat exchangers (HPHEs) are capable of transferring large amounts of heat over relatively large distances while operating within small temperature differences between the heat source and heat sink. HPHEs are popular due to the fact that they are efficient and function passively. They are used in various applications such as waste heat recovery from hot exhaust flue gas or to replace the wrap around coil in an air conditioning system.

A thermosyphon is a wickless heat pipe. A compact and easy to install “in-line” or “C-shape” thermosyphon, CST is shown in Fig. 1. It consists of two banks of single or multiple rows of thermosyphons with each set of pipes bent into a C-shape. The CSTs are then retrofitted around the conventional cooling coil of a refrigerating vapour compression machine. The CST is designed for easy installation and retro-fitting into existing air conditioning units. In order to allow for water condensate to run off, this physical configuration would require the coil to be placed with the condenser section slightly off-set to either side of the evaporator section. The slope angle of the CST is defined as the angle  $\theta$  measured from the horizontal of the plane containing the thermosyphon, Fig. 1.

## 2. Literature survey

Jouhara (2009) analyzed the energy and cost saving potential quantitatively with the use of a 3m<sup>3</sup>/s air flow CST system. Simulation of different conditions was performed by varying the outside air conditions and supply air temperature. He showed that an annual savings of nearly 134MWh could be achieved with the additional set up cost of the CST being marginal after taking into account the reduction in size of other equipment and operating energy cost. The return of investment in terms of the energy savings is estimated to be around 1 month. Jouhara and Meskimmon (2010) studied experimentally the effect of air flow velocity on the thermosyphon effectiveness using a 7-loop single-row R134A charged CST. Tests were conducted using a 15kW electric heater located between the condenser section and evaporator section in order to reverse the temperature difference imposed upon the pre-cool and reheat coils. From their experiment with six different volumetric air flow rates, they discovered that the effectiveness increased with air velocity. Jouhara and Ezzuddin (2013) investigated a CST using R134A as the fill liquid. The test unit consisted of a two-pass evaporator section as well as a two-pass condenser section using 330mm long x 11.2 mm diameter bare copper tubes. The evaporator was heated using resistance wires between 50 – 500W, and the condenser was cooled using coolant water at flow

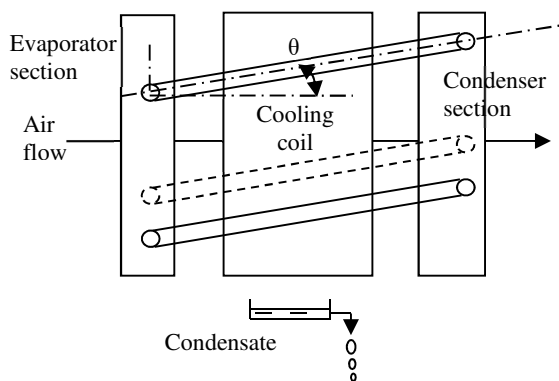


Fig. 1. C-shape thermosyphon heat exchanger.

\* Corresponding author. Email: [skong@utar.edu.my](mailto:skong@utar.edu.my)

rates between 3-13 mm<sup>3</sup>/s. Their results indicated that the vapour flowed from the upper evaporator pipe to the upper condenser pipe and then flowed back down through the lower condenser pipe back to the lower evaporator pipe. The thermal resistance of the thermosyphon decreased as power increased, reaching a peak of 0.048°C/W at 250W.

Hill and Jeter (1994) examined the use of a HPHE for enhanced dehumidification. They evaluated the air conditioning performance through a combination of HPHE thermal node model and a model for air conditioning system. They observed a significant increase in dehumidification capacity as well as nominal reduction in sensible heat ratio. El-Baky and Mohamed (2007) tested the use of a HPHE for heat recovery in air conditioning. They varied the ratio of mass flow rate between the return air and fresh air. Their results showed that the fresh and return air temperatures and effectiveness increased with the increase in fresh air inlet temperature. They concluded that an optimum effectiveness could occur when the fresh air inlet temperature was near the fluid operating temperature of the heat pipe.

Zhao et al. (2006) studied a CST system under various air flow rates, dry bulb temperatures and relative humidity. The reported energy savings varied between 11.8 – 30.3% but decreased an increase in supply air inlet temperature, air relative humidity and air quantities. Beckert and Herwig (1996) studied the effect of inclination on the overall performance of an inclined six-row 19 pipes/row R22 filled thermosyphon HPHE. They discovered that the overall performance was still acceptable even up to 6° inclination. The maximum recorded hot air temperature was at 55°C while the cold air supply temperature was between 17 – 29 °C. Jouhara et al. (2013) investigated a thermosyphon using ethanol-water azeotrope as fill liquid at the fill ratio of 0.5. The thermosyphon was structured such that a 400 mm long water cooled condenser was inclined (12°) and attached to a horizontal 1000 mm long evaporator which was electrically heated to 0.8 kW. The unit was observed to perform satisfactorily at different inclinations of the evaporator section from 0° – 90°.

Hagens et al. (2007) compared the performance of conventional plate-type exchangers and a 4-row R134A filled thermosyphon HPHE. A water-air heat exchanger was used to heat the air between the condenser section and evaporator section. Test results showed that the heat transfer coefficients for the evaporator and condenser section approximately 10-40W/m<sup>2</sup> K and 20-50W/m<sup>2</sup> K respectively. This shows that the thermosyphon HPHE can be used as a substitute for water cooled heat exchanger without loss in performance. Meskimmon (2004) simulated an air conditioning system utilizing 100% outside make up air with and without the CST under hot and humid climate. His simulation showed that there were significant energy savings. He advised caution when the CST is considered for extreme applications where latent and sensible load vary greatly as the heat pipes may take up large space and high cost.

A wickless heat pipe is also known as a thermosyphon. Ong (2011) investigated the performance of R134A and R410A-filled thermosyphons at low temperature. A copper pipe with 38 mm O/D and 32 mm I/D was used to fabricate the thermosyphon. The evaporator, condenser and adiabatic lengths were 405 mm, 327 mm and 110 mm long, respectively. The fill ratio used for both refrigerants were 0.5 and 0.7. He concluded that there was no significant difference between the performance of the R134A- and R410A-filled thermosyphon and that the mean evaporator and condenser heat transfer coefficients were independent of fill ratio and inclination. Ong et al. (2014) compared the performance of a 760 mm long, 38 mm O/D x 32 mm I/D copper pipe thermosyphon filled with R410A and water at various fill ratios and inclinations. The evaporator, adiabatic and condenser section were 390 mm, 90 mm and 327 mm long, respectively. They concluded that the axial wall temperature distribution was not uniform and increased with increasing input power. Dry out was observed at high input power, low fill ratio and high inclinations. It was also observed that the R410A thermosyphon performed better in a vertical position at all fill ratios and that the water-filled thermosyphon performed better at low fill ratio and at an inclined position.

### 3. Objective

There are only a few studies conducted on the performance of the C-shape thermosyphon (CST), and even lesser studies on the use of R410A as fill liquid. The objective of this paper is to determine experimentally the thermal performance of a R410A filled CST and in particular the effect of the slope on its performance.

## 4. Experimental Investigation

### 4.1 Experimental apparatus and procedure

The experimental set-up is shown schematically in Fig. 2. The thermosyphon was fabricated from a 12.7 mm O/D x 9.52 mm I/D copper tube bent into the shape of a “C”. The evaporator, condenser and adiabatic sections were each 310 mm long. The condenser section was fitted with a concentric 310 mm long x 30mm O/D copper water jacket. A brass “T-piece” brazed at the end of the condenser section was fitted with a charging valve to allow for vacuuming/charging of the thermosyphon and to fit a thermocouple to measure the saturation temperature inside. Heating at the evaporator section was applied via nichrome wire wound around the entire evaporator section and connected to an AC transformer. Applied voltage (V) and current (A) were measured using a voltmeter and an ammeter. Input power (P) was calculated from the product of V x A. The condenser and adiabatic sections were insulated with 25 mm thick “insulflex” insulation. The evaporator section was insulated with 50 mm thick rock wool.

Type T copper-constantan thermocouple wires ( $\pm 0.5^\circ\text{C}$ ) were mechanically attached to the surface of the thermosyphon at the locations shown in Fig. 2 to measure the surface temperature at the evaporator ( $T_{e1} - T_{e4}$ ), adiabatic ( $T_{ad1} - T_{ad2}$ ) and condenser ( $T_{c1} - T_{c2}$ ) sections. Additional thermocouples were employed to measure the coolant water inlet ( $T_{wi}$ ) and outlet ( $T_{wo}$ ) temperatures. A thermocouple probe inserted into the thermosyphon at the cross-head brass fitting measured the saturation temperature ( $T_{sat}$ ) of the thermosyphon. Saturation pressure ( $P_{sat}$ ) was measured with a digital pressure transducer. Ambient temperature ( $T_{amb}$ ) was measured using another type T thermocouple probe located near to the equipment. The ambient was not controlled in the air conditioned laboratory and varied by about  $\pm 2^\circ\text{C}$  throughout the experiments.

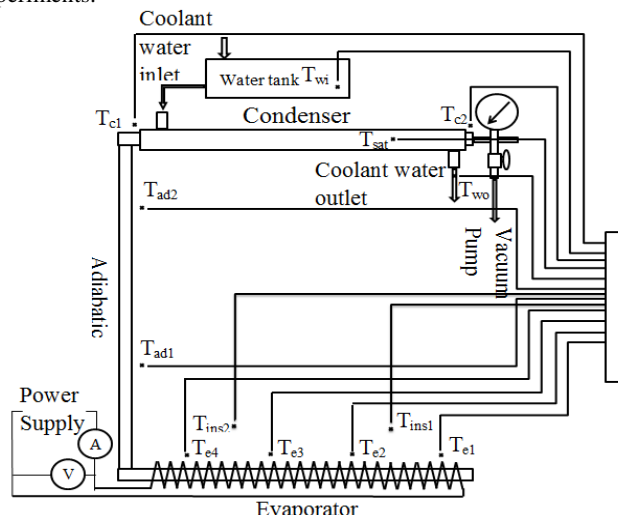


Fig. 2. Schematic of experimental set-up.

Coolant water mass flow rate was determined by measuring the amount of water discharged with a stop watch. Coolant water flow rate was maintained at 0.05 kg/s. Coolant water temperature was not controlled and it varied from 24°C - 27°C through the experiments. The high flow rate employed resulted in a near uniform temperature at the condenser section but with a low temperature rise across the cooling

water jacket. Hence the heat transfer rate to the condenser was assumed equal to the power input at the evaporator. All data were recorded on a data logger at one minute intervals. A photograph of the experimental set up is shown in Fig. 3.

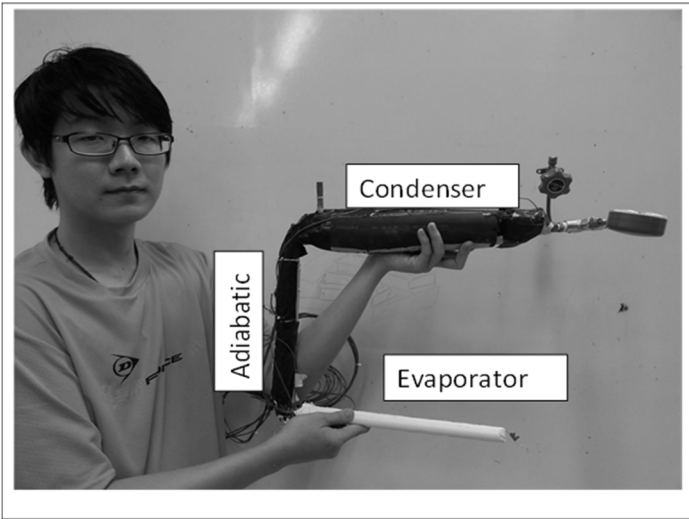


Fig. 3. Photograph of experimental set-up.

The CST was first vacuumed before being filled with the required amount of R410A refrigerant to achieve a fill ratio (FR) of 1.00. Experiments were carried out with various angles of  $\theta$  from 30°, 60° and 90° and heating power (P) from 40W to 100W in steps of 20W. Each experiment was repeated three times to ensure consistency and repeatability. Mean evaporator ( $T_{em}$ ) and condenser ( $T_{ec}$ ) section temperatures were assumed to be equal to the arithmetic mean of the probes in the respective sections.

4.2 Experimental results

The results were found to be repeatable to within  $\pm 2^\circ\text{C}$ . Typical results of temperature distribution along the thermosyphon wall, saturation, coolant water, insulation and ambient temperatures are shown in Figs. 4 – 6 at various power inputs and  $\theta = 90^\circ, 60^\circ$  and  $30^\circ$ , respectively. The results showed that the temperature distribution along the evaporator section was quite uniform at the power inputs applied from 40-100W. The temperature decreased towards the adiabatic and condenser sections. The adiabatic section exhibited nearly uniform temperature. The temperatures at both ends of the condenser section were nearly equal. The saturation temperature was less than the evaporator section temperature and higher than the condenser temperature as expected. All temperatures increased as input power increased. The temperature along the evaporator section is higher than that along the condenser section. Coolant water increased in temperature as a result of heat transfer from the evaporator section. However, with the high coolant flow rate adopted, the actual amount of heat transferred could not be accurately determined. It was assumed that the heat transport across the CST was equal to the input power as insulation temperature showed that the insulation effect was very good, less than 4% heat loss.

Figs. 7 – 10 show the effect of slope angle ( $\theta$ ) at the various power inputs from 100 W to 40 W, respectively. The temperature distribution profile at 90° and 60° were quite similar. However, it was observed that at 30°, the temperatures were higher than those obtained at 90° and 60° by a few degrees. This was attributed to partial burn-out in the evaporator section due to the inability of the condensate to flow back down fast enough towards the evaporator section from the upper condenser section because of the slope of the thermosyphon. The condenser and evaporator were equal in volume.

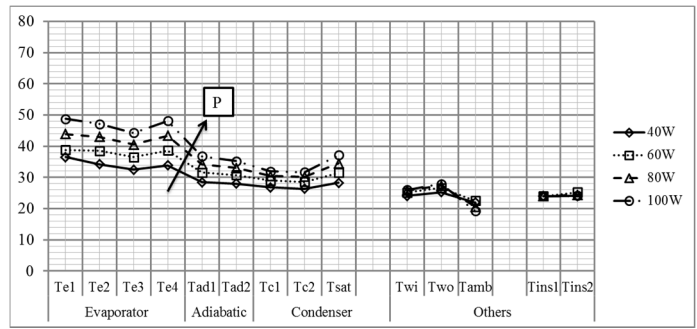


Fig. 4 Temperature distribution at  $\theta = 90^\circ$

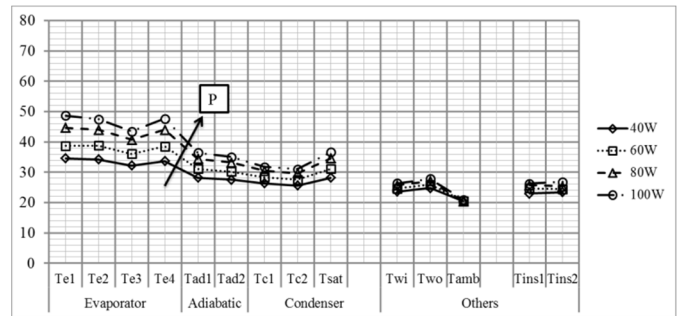


Fig. 5 Temperature distribution at  $\theta = 60^\circ$

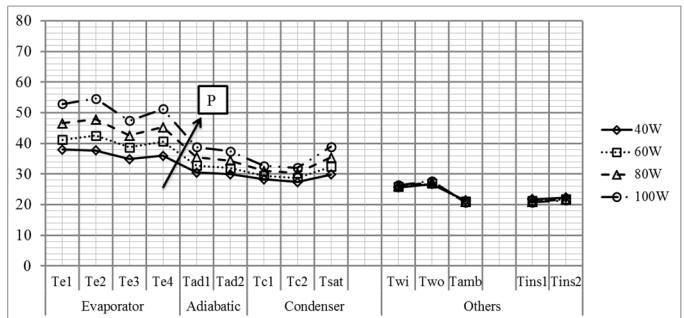


Fig. 6 Temperature distribution at  $\theta = 30^\circ$

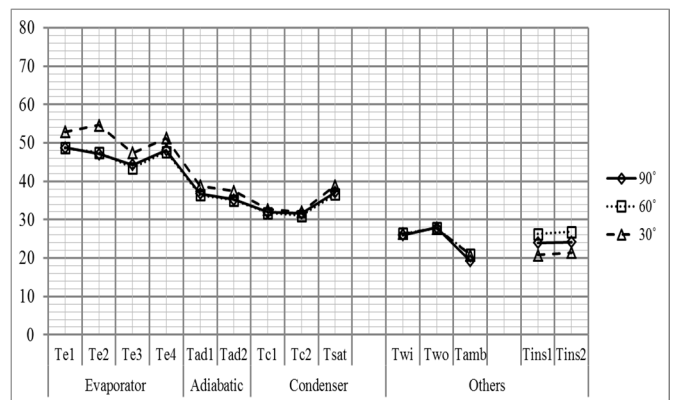


Fig. 7 Temperature distribution at P = 100W

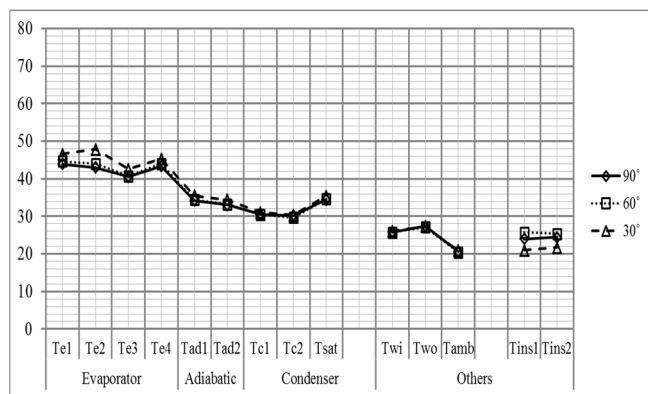


Fig. 8 Temperature distribution at P = 80W

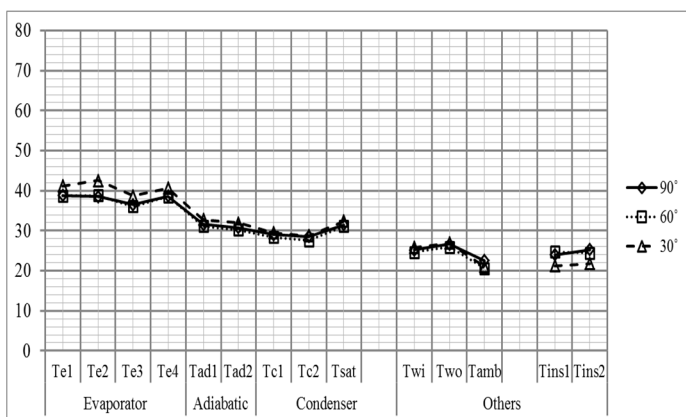


Fig. 9 Temperature distribution at P = 60W

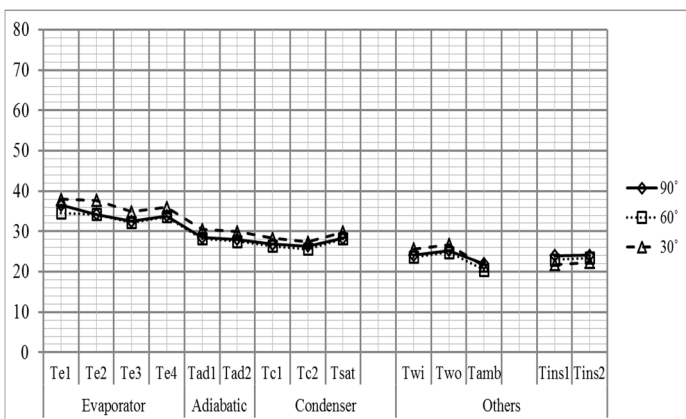


Fig. 10 Temperature distribution at P = 40W.

The performance of a thermosyphon could be gauged from Fig. 11 which shows the results of input power (P) plotted against temperature difference between evaporator and condenser ( $\Delta T_{ec}$ ) at the various  $\theta$  from  $30^\circ - 90^\circ$ . The regression lines obtained are quite linear with regression coefficients greater than 0.98. The results show that it required a temperature difference of about 2 to  $3^\circ\text{C}$  in order for the thermosyphon to work. The results at  $90^\circ$  and  $60^\circ$  agreed to within  $\pm 0.5^\circ\text{C}$ . However, the results at  $30^\circ$  showed that it differed from the others by as much as  $3.5^\circ\text{C}$  at 100 W.

The experimental value of the thermal resistance of the thermosyphon is calculated from

$$R_{hp} = \Delta T_{ec} / P \quad (1)$$

The theoretical thermal resistance of the CST can be calculated using

$$R_{hp} = \frac{\ln(D_o/D_i)}{2\pi k_{wall} L_{evap}} + \frac{\ln(D_o/D_i)}{2\pi k_{wall} L_{cond}} + \frac{1}{h_{evap} \pi D_i L_{evap}} + \frac{1}{h_{cond} \pi D_i L_{cond}} \quad (2)$$

Figure 12 shows the results of the C-shape pipe thermal resistance ( $R_{hp}$ ) plotted against temperature difference ( $\Delta T_{ec}$ ). The results showed that the thermal resistance decreased slightly with increasing input power and remained quite constant at about  $0.17 \pm 0.2 \text{ K/W}$  from 60-100 W. The thermal resistance for pipes sloped at  $60^\circ$  and  $90^\circ$  show very little differences between them. Thermal resistance for the  $30^\circ$  slope pipe was about  $0.03 \text{ K/W}$  higher than for the others.

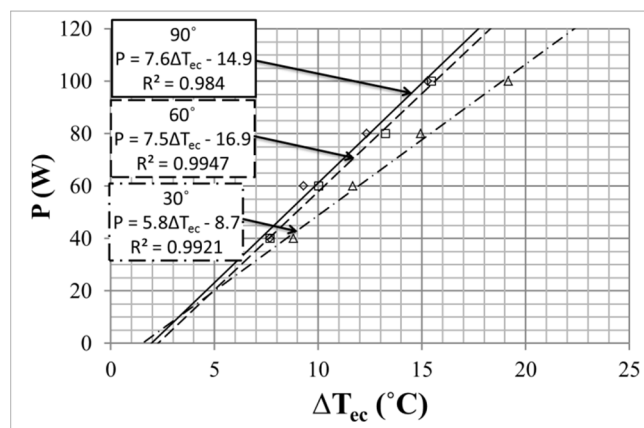


Fig. 11 Performance of R410A filled thermosyphon.

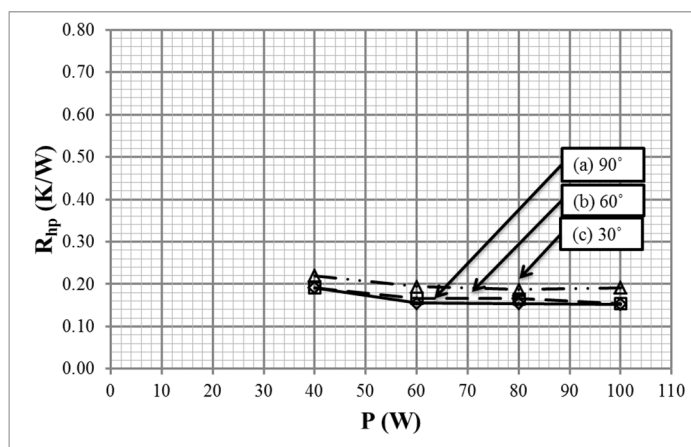
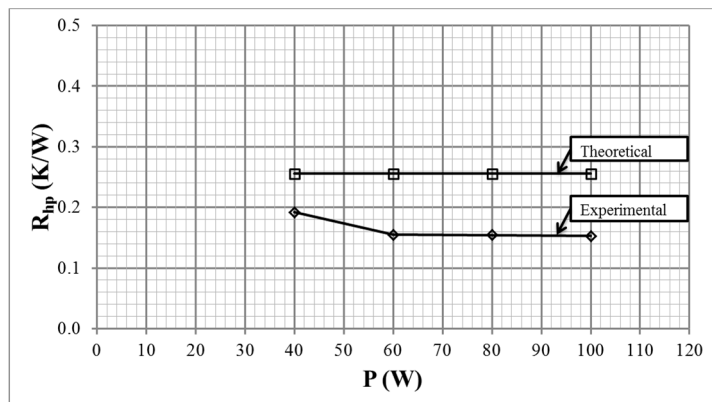


Fig. 12 Thermal resistance obtained at various slopes.

Evaporating and condensing heat transfer coefficients for a straight vertical thermosyphon with similar diameter and evaporator and condenser lengths as the present CST unit and filled with R410A were determined from an earlier experiment [Ong et al. (2016)]. The evaporating heat transfer coefficients were found to vary from  $587 \text{ W/m}^2 \text{ K}$  at 40 W to  $767 \text{ W/m}^2 \text{ K}$  at 100 W. The condensing heat transfer coefficients varied from  $1101 \text{ W/m}^2 \text{ K}$  at 40 W to  $1186 \text{ W/m}^2 \text{ K}$  at 100 W. Substituting average values of  $623 \text{ W/m}^2 \text{ K}$  and  $1086 \text{ W/m}^2 \text{ K}$  for evaporating and condensing heat transfer coefficients, respectively into Eqn. (2), the theoretical thermal resistance ( $R_{hp}$ ) of the present CST is calculated and compared with the experimental results in Fig. 13. The theoretical individual thermal resistances calculated are as follows: wall resistance =  $0.004 \text{ K/W}$ , evaporator side =  $0.156 \text{ K/W}$  and condenser side =  $0.099 \text{ K/W}$ . This shows that the dominant resistance is contributed from evaporator resistance. The overall or total thermal resistance is

equal to 0.256 K/W. The experimental thermal resistance from Eqn. (1) is determined from the temperature difference ( $\Delta T_{ec}$ ) obtained. From Fig. 11, the experimental value of  $\Delta T_{ec}$  is about 15°C for the 90° slope CST at 100 W. The accuracy of the thermocouples is within  $\pm 0.5^\circ\text{C}$  and the power measured are within  $\pm 2$  W, the experimental accuracy is to within  $\pm 10\%$ . Hence the experimental value of  $R_{hp} = 0.150 \pm 0.015$  K/W. A comparison of the theoretical and experimental results shows that the predicted value is greater than experimental by about 0.10 K/W. The simple model proposed could only be employed to provide an approximate thermal resistance for the CST.

Further work needs to be performed to determine the effects of other fill liquids, input power and aspect ratios (length/diameter). A flow visualization study would enable dry-out conditions to be observed.



**Fig. 13** Comparison of experimental and theoretical thermal resistances for R410A-filled C-shape thermosyphon.

## 5. CONCLUSIONS

The performance of a C-shape thermosyphon filled with R410A was determined at various power inputs and slope angles. There were no differences in performances obtained with slope angles between 60-90°. Performance decreased when slope was at 30°. Aspect ratio of the thermosyphon could affect its performance. The simple model could provide an approximate value for the thermal performance of the CST.

## NOMENCLATURE

|                     |   |
|---------------------|---|
| $\theta$            | Slope angle ( $^\circ$ )                                    |
| P                   | Input power (W)   |
| $T_{e1} - T_{e4}$   | Evaporator temperature ( $^\circ\text{C}$ )                 |
| $T_{ad1} - T_{ad2}$ | Adiabatic temperature ( $^\circ\text{C}$ )                  |
| $T_{c1} - T_{c2}$   | Condenser temperature ( $^\circ\text{C}$ )                  |
| $T_{wi}$            | Coolant water inlet temperature ( $^\circ\text{C}$ )        |
| $T_{wo}$            | Coolant water outlet temperatures ( $^\circ\text{C}$ )      |
| $T_{ad}$            | Mean temperature of adiabatic section ( $^\circ\text{C}$ )  |
| $T_{em}$            | Mean temperature of evaporator section ( $^\circ\text{C}$ ) |
| $T_{cm}$            | Mean temperature of condenser section ( $^\circ\text{C}$ )  |
| $\Delta T_{ec}$     | $= (T_{em} - T_{ec})$ ( $^\circ\text{C}$ )                  |
| $T_{sat}$           | Saturation temperature ( $^\circ\text{C}$ )                 |
| $T_{amb}$           | Ambient temperature ( $^\circ\text{C}$ )                    |
| $R_{hp}$            | Thermal resistance (K/W)                                    |
| $D_o$               | Outer diameter = (0.0127m)                                  |
| $D_i$               | Inner diameter (= 0.0095m)                                  |
| $k_{wall}$          | Thermal conductivity of copper wall (= 100W/m K)            |
| $L_{evap}$          | Length of evaporator section (= 0.310m)                     |
| $L_{cond}$          | Length of condenser section (= 0.310 m)                     |

|            |   |
|------------|---|
| $h_{evap}$ | Evaporator heat transfer coefficient (W/m <sup>2</sup> K) |
| $h_{cond}$ | Condenser heat transfer coefficient (W/m <sup>2</sup> K)  |

## REFERENCES

- Jouhara, H., 2009, "Economic Assessment of the Benefits of Wraparound Heat Pipes in Ventilation Processes for Hot and Humid Climates," *International Journal of Low-Carbon Technologies*, 4, 52-60. <http://dx.doi.org/10.1093/ijlct/ctp006>
- Jouhara, H., and Meskimmon, R., 2010 "Experimental Investigation of Wraparound Loop Heat Pipe Heat Exchanger used in Energy Efficient Air Handling Units," *Energy*, 35, 4592 – 4599. <http://dx.doi.org/10.1016/j.energy.2010.03.056>
- Jouhara, H., and Ezzuddin, H., 2013, "Thermal Performance Characteristics of a Wraparound Loop Heat Pipe (WLHP) Charged with R134A," *Energy*, 61, 128 – 138. <http://dx.doi.org/10.1016/j.energy.2012.10.016>
- Hill J.M., and Jeter, S.M., 1994 "The Use of Heat Pipe Heat Exchangers for Enhanced Dehumidification," in *Trans. ASHRAE 100(1)*, New Orleans, LA, 91 - 102.
- Mostafa A. Abd El-Baky and Mousa M. Mohamed, 2007, "Heat Pipe Heat Exchanger for Heat Recovery in Air Conditioning," *Applied Thermal Engineering*, 27, 795-801. <http://dx.doi.org/10.1016/j.applthermaleng.2006.10.020>
- Zhao, X., Li, Q., and Chao Yun, 2006, "Performance Test and Energy Saving Analysis of a Heat Pipe Dehumidifier," in *Proc. 6th International Conference Enhanced Building Operations, ESL-IC-11-97*, Shenzhen, China, 1-4.
- Beckert, K., and Herwig, H., 1996, "Inclined Air to Air Heat Exchangers with Heat Pipes: Comparing Experimental Data with Theoretical Results," *IEEE*, 96068, 1441 – 1446. <http://dx.doi.org/10.1109/IECEC.1996.553937>
- Jouhara, H., Ajjji, Z., Koudsi, Y., Ezzuddin, H., and Mousa, N., 2013, "Experimental Investigation of an Inclined-Condenser Wickless Heat Pipe Charged with Water and an Ethanol-water Azeotropic Mixture," *Energy*, 61, 139 – 147. <http://dx.doi.org/10.1109/IECEC.1996.553937>
- Hagens, H., Ganzevles, F.L.A., van der Geld, C.W.M., and Grooten, M.H.M., 2007, "Air Heat Exchangers with Long Heat Pipes: Experiments and Predictions," *Applied Thermal Engineering*, 27, 2426-2434. <http://dx.doi.org/10.1016/j.applthermaleng.2007.03.004>
- Meskimmon, R., 2004, "Heat Pipes for Enhanced Dehumidification," in *SPC coil products, Application Notes 002.*, 1-24.
- Ong, K.S., 2011, "Effects of Inclination and Fill Ratio on R134a and R410A," *Journal of Energy, Heat and Mass Transfer*, 33, 145 – 152.
- Ong, K.S., Tong, W.L., Gan, J.S., and Hisham, N., 2014, "Axial Temperature Distribution and Performance of R410A and Water filled Thermosyphon at Various Fill Ratios and Inclinations," *Frontiers in Heat Pipe*, 5(2), 1 – 7. <http://dx.doi.org/10.5098/fhp.5.2>
- Ong K.S., Goh, Gabriel., Tshai, K.H., Chin, W.M., 2016, "Thermal resistance of a thermosyphon filled with R410A operating at low evaporator temperature" *Applied Thermal Engineering*, 106, 1345 – 1351. <http://dx.doi.org/10.1016/j.applthermaleng.2016.06.080>